J. Chem. Sci. (2020) 132:53
https://doi.org/10.1007/s12039-020-1755-x

REGULAR ARTICLE

Sulfur Nested with Mixture of MnO_2/AB Composite as Efficient Host for High-Performance Li–S Batteries

G RADHIKA, R SUBADEVI and M SIVAKUMAR*
#120, Energy Materials Lab, Department of Physics, Science Block, Alagappa University, Karaikudi, Tamil Nadu 630 003, India
E-mail: susiva73@yahoo.co.in

MS received 1 September 2019; revised 1 December 2019; accepted 2 December 2019

Abstract. Lithium–sulfur (Li–S) batteries have established a tremendous interest in recent years because of their high specific capacity (1675 mAh g^{-1}) and energy density (2600 Wh kg^{-1}). In the present work, the electrode comprising carbon source viz., Acetylene Black (AB) and Manganese Oxide (MnO_2) to serve as an efficient sulfur host in two different ratios (MnO_2:AB as 10:20 (M1) and 20:10 (M2)) for Li/dissolved polysulfide batteries. The composite was characterized and studied by X-ray diffraction (XRD), Raman Spectroscopy, Nitrogen adsorption/desorption measurements, High-resolution transmission electron microscopy (HRTEM), X-ray photon spectroscopy (XPS), Thermogravimetric analysis (TGA) and electrochemical performance such as cyclic voltammetry (CV) and charge–discharge (C/D) tests. It shows good cycle performance and exhibits an initial capacity of 1540 mAh/g at 0.1 C between 1.5 and 3.0 V for MnO_2 rich sample. Performance enhancement was also brought about by the adsorptive properties of MnO_2 which help in locking the polysulfide discharge products within the cathode structure.

Keywords. Composites; metal oxide; lithium–sulfur; acetylene black; energy storage.

1. Introduction

Among the several existing energy sources, rechargeable lithium-ion batteries have undergone significant progress in the recent decades as power sources for various portable devices such as laptops, smartphones and electric vehicles.[1–4] Lithium-ion batteries are not sufficient to meet the increasing demands of energy storage devices including transport and power grid applications.[5] Newfangled rechargeable batteries with high charge storage capacities and prolonged performance have been developed. Of that, rechargeable lithium–sulfur (Li–S) batteries possess the high specific capacity and theoretical energy density building them efficient entrants for the energy storage systems. Furthermore, Sulfur (S) is abundant and eco-friendly. Li–S batteries have gleaned worldwide interest in the emerging large-scale energy storage applications. Despite its benefits, Li–S batteries have some shortcomings. The insulating nature of sulfur and its discharged products, which un-enviably lower the utilization of the active material and poignant the electrochemical performance of the battery; the major problem is the dissolution of the lithium polysulfide intermediates, in an electrolyte, causing irrevocable loss of active materials and impoverished cycle performance.[6]

In order to enhance the electronic conducting property of sulfur and also to inhibit the deficit of the active substances and aggrandize the reversibility of sulfur material, diverse composite materials, like porous carbon, metal–organic frameworks (MOFs),[7,8] metal oxide,[9,10] and conductive polymer [11,12] have been designed and prepared. Therefore, the carbon materials, with high electronic conductivity, low mass density and copious porous structure, have been extensively investigated to discourse abovementioned defies of the sulfur electrode.[13–15] Recently, MOFs have garnered great interest with ion exchange properties and their sorption capacities are perceived to be considerably superior to conventional materials.[16–18] Carbon materials are exposed to be more effective

*For correspondence

Electronic supplementary material: The online version of this article (https://doi.org/10.1007/s12039-020-1755-x) contains supplementary material, which is available to authorized users.

Published online: 12 March 2020

owing to its good electrical conductivity, large pore volume, and strong microporous adsorption capability to improve the cycle stability, active sulfur utilization and high-rate capability of the sulfur cathode.[20] Among these materials, the metallic oxide is engrossing whereas it caters to higher electrode density than carbon materials as well as analogous diffusion of Li in the structure. Newly, metallic oxides such as TiO_2, SiO_2, and MnO_2[21] have been hired for lithium−sulfur batteries.[22]

Of these, MnO_2-based composites with a uniform structure, earth-abundant and large surface area have been attracting particular attention towards the ability to adsorb lithium polysulfides and facilitate the lithium-ion diffusion.[23] Recently, Hou[24] and Lou[25] developed a highly efficient sulfur host materials with hollow carbon nano boxes (HCB) and hollow carbon nanofibers (HCF) filled with birnessite-type MnO_2 nanosheets for the combination of physical and chemical entrapment of Lithium polysulfides.

MnO_2/AB was chosen as a sulfur host matrix material due to MnO_2 can effectively adsorb lithium polysulfides thereby preventing dissolution; minimize "shuttle effect" and significantly improving cycle performance. Therefore, in this paper, the performances of the composites are compared by varying the ratio of MnO_2 and AB with sulfur. This intention considerably improves the electrical conductivity and pontificate the insulating nature of the S cathode. Furthermore, the adsorption of the soluble polysulfides and transportation of Li-ions is enhanced.

2. Experimental

2.1 *Material preparation*

Sulfur (Alfa Aesar), MnO_2 (Alfa Aesar) and Acetylene black (Alfa Aesar) were mixed with 70:10:20 (SMC1) and 70:20:10 (SMC2) ratio and manually grounded for 1 h in an agate mortar and were heat-treated at 155 °C for 20 h in a sealed vessel filled with argon gas. After cooling down to room temperature, SMC1 and SMC2 composites were obtained.

2.2 *Material characterization*

Thermogravimetric analysis (Perkin Elmer, Diamond TG) was performed in determining the sulfur degradation information of the sample. The crystalline phase of the sample has been identified by Powder X-ray diffraction (PANalytical XPERT-PRO with Cu Kα radiation) using CuKα radiation. The morphological study has been employed by high-resolution transmission electron microscopy (jeol/JEM 2100). Brunauer–Emmett–Teller measurements (QUADRASORB SI) were examined to measure the surface area and pore size of the composites. RAMAN spectroscopy (SEKI focal) Analysis was employed to classify the vibration modes in the composites. X-ray photoelectron spectroscopy [ESCALAB 250 xi, Thermo Scientific) measurements were taken with ultrahigh vacuum setup with monochromatic detector to identify the material and their binding energies.

2.3 *Electrochemical measurements*

Coin-type (CR2032) cells were prepared using polypropylene separator between a cathode and lithium metal foil in the glove box. Electrodes are made with these composites by doctor blade system. The slurry consisted of 70 wt.% active material, 20 wt.% Super P and 10 wt.% poly(vinylidene fluoride) (PVdF) dissolved in N-methyl 2-pyrrolidinone was coated on the foil, roll-pressed and cut into circular discs and dried under vacuum at 60 °C for 12 h. Coin-type (CR2032) cells were massed in an argon-filled glove box to avoid contamination by moisture and oxygen. 1 M lithium bis(-trifluoromethane sulfonyl)imide in a solvent mixture of DOL (1,3-dioxolane): DME (dimethoxyethane) (1:1, v/v) containing 0.05 M $LiNO_3$ were used as the electrolyte.

3. Results and Discussion

The thermal history of the as-prepared SMC2 composite has been analyzed by Thermogravimetric analysis (TG) under Ar environment as shown in Figure S1 (Supplementary Information). It can be seen that the sulfur mass stays stable up to 190 °C. When the temperature increased beyond this, the mass of sulfur decreased to zero when it reaches 350 °C, which is ascribed to the complete melting of sulfur. The residue observed in the TGA curve of the composite SMC2 is corresponding to the carbon source and MnO_2. Thus, mass loss of sulfur in composite was around 70% and the curves remain stable when the composites are heated over 400 °C due to vaporization of sulfur from the mesopores of the composite.[19,20]

Figure 1(a, b & c) shows the XRD patterns of pure sulfur, SMC1 and SMC2 composite. The XRD pattern of pure sulfur is well in agreement with the JCPDS (77-0145). In Figure 2(b), the sharp diffraction peak at $2\theta = 23°$ of the SMC1 and SMC2 composites indicates that the sublimed sulfur exists in a crystalline state. In addition to MnO_2 peaks (JCPDS (24-0735)), the diffraction peak intensity of sulfur in SMC1 and SMC2 composite decreases when compared to bare

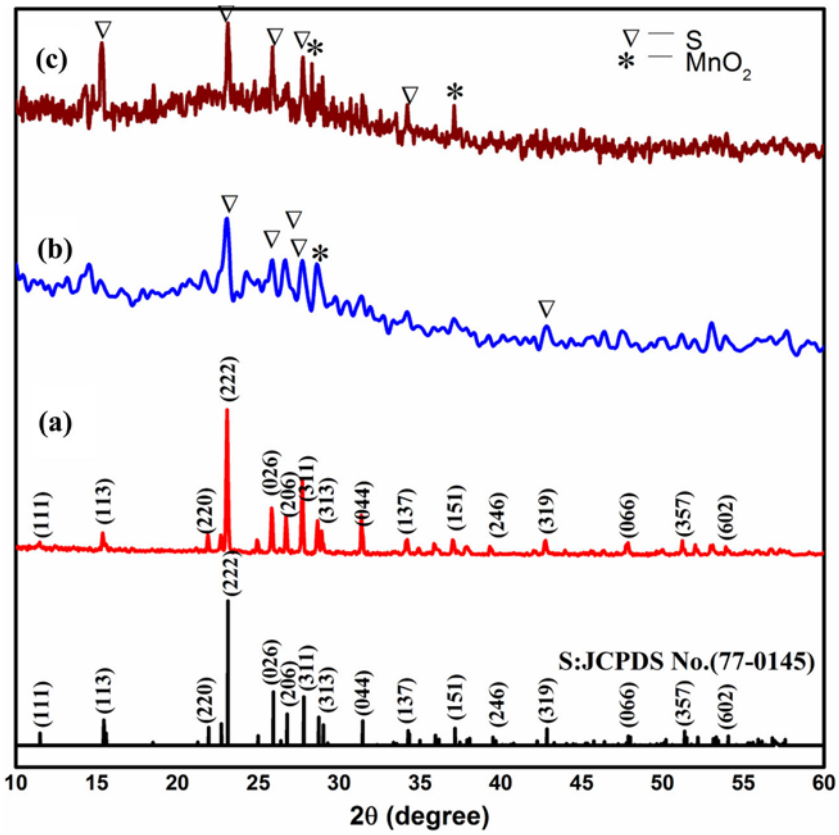

Figure 1. XRD pattern of (a) pure sulfur (b) SMC1 (c) SMC2 composite.

sublimed sulfur, thereby indicating that most of the sulfur is well-dispersed in the composite.[26,27] Therefore, the peaks of sulfur were not altered structures of the composites. It signifies that there is an absence of chemical reaction between the composite upon heat treatment.[28,29]

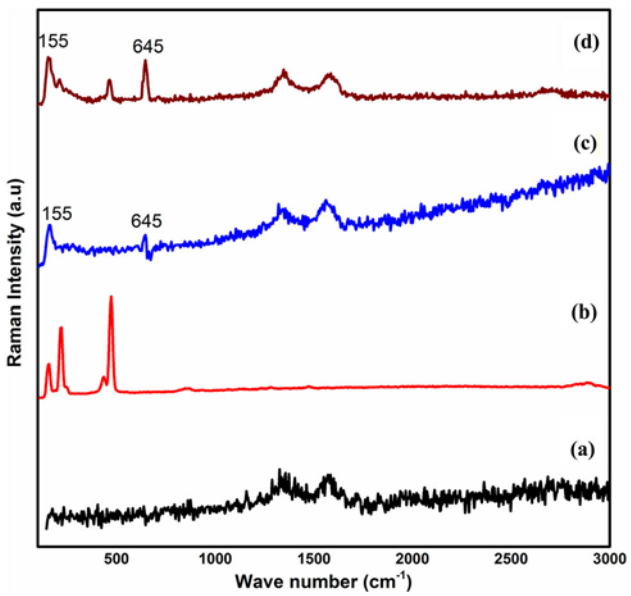

Figure 2. RAMAN spectra of (a) Acetylene Black (b) pure sulfur (c) SMC1 (d) SMC2 composite.

Figure 2(a–d) shows Raman spectra of pure AB, sulfur and SMC1 and SMC2 composites. In Figure 3(b), the carbon source exhibits two Raman bands at 1350 and 1567 cm^{-1}, respectively. The Raman band at 1350 cm^{-1} is attributed to the disordered (D) band and is linked with defects in the structure.[31] The other Raman band at 1567 cm^{-1} is attributed to graphitic (G) band and is associated with the vibration of any pair of sp^2 sites inside the graphitic pattern.[26] These bands appear at 1346 and 1580 cm^{-1} in the composites, which is clearly visible in Figure 3(c & d), the characteristic peaks of MnO_2 and sublimed sulfur has been observed at 645 and 150 cm^{-1} respectively in the composites. Raman bands with high intensity at 153, 219 and 472 cm^{-1} are corresponding to aggregated sulfur. In contrast with sulfur, SMC2 does not exhibit those Raman bands with high intensity, which results from the dispersed state of sulfur in the composite.[30]

Brunauer–Emmett–Teller (BET) analysis has been employed to calculate the specific surface area of SMC1 and SMC2 composite were illustrated in Figure S2(a), Supplementary Information. BJH pore size

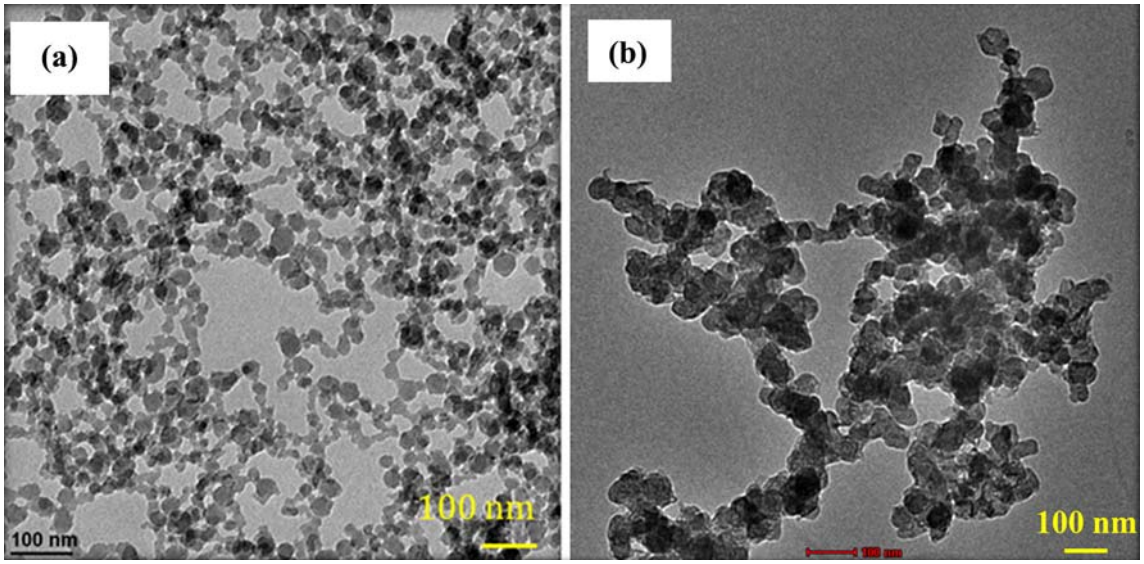

Figure 3. TEM images of (a) SMC1, (b) SMC2 composite.

distributions of MnO_2 are shown in supporting information Figure S2(b) implies that most of the pores are below 5 nm. It indicates that the MnO_2 possess a mesoporous nature. However, SMC2 sample does not exhibit a typical isotherm, which elucidates that the sulfur particle almost completely covers the surface of the composite as compared to the SMC1 composite.

Figure 3(a) shows TEM images of the SMC1 composite cathode material in different magnification. It is found that the particles of AB intermingle to form chain-like structures,[32] which is evident from the good conductivity of the AB matrix. The fact that some shallow of the AB matrix is still clean without sulfur deposition indicates that the sulfur is not dispersed homogeneously. From Figure 3(b), the SMC2 cathode material shows that the sulfur particles are uniformly dispersed into the porous structure of the host matrix. The images of SMC2 composite signify that there is no sulfur accretion on the surface of AB implies the sulfur is infiltrated into the pores of AB.[30]

XPS analysis of the survey performed from 0 to 700 eV to identify the elemental composition of the SMC2 composite sample, which reveals the presence of Mn, C, S and O elements; specifically, the peaks located at 163, 228, 284, 531.10 and 643.9 eV corresponds to S2p, S2s, C1s, O1s and Mn 2p, respectively as shown in Supplementary Information, Figure S3.[33,34] XPS spectra of S2p and Mn $2p_{3/2}$ were used to examine the cathode before cycling, as shown in Figure 4(a & b). From Figure 4(a), it is observed that the multiple S2p spectra attributed to various valence states of sulfur. The peak at 164 eV is ascribed to S–S bonds from elemental sulfur; the other peaks between 166 and 170 eV are connate to the existence of SO_4^{-2} or S_2O_3, which may cause by the oxidation of sulfur upon heating.[18] In Figure 4(b) the Mn $2p_{1/2}$ and Mn $2p_{3/2}$ spectra of the cathode shows typical peaks of the MnO_2, which has strong multiple peaks between 642 and 653 eV corresponding to Mn^{3+} in SMC2 composite.[35,36]

Figure 5(a & b) shows the initial cycle, 10th, 20th, 30th, 40th and 50th galvanostatic charge–discharge profiles of the SMC1 and SMC2 system. During the cycling process, the composite electrodes show typical charge–discharge potential plateaus in the voltage profile which confirmed the two-step reaction of sulfur with lithium and it is good agreement with the CV results.[26] The initial discharge capacity of the SMC1 composite cathode was 1350 mAh g^{-1}. In the subsequent cycling, the discharge capacity of SMC1 composite cathode was reduced to 1305 mAh g^{-1}, with an irrevocable capacity loss. It is noted that the capacity loss in the beginning cycles, the effect is escorted by the expansion of sulfur and redistribution of the active sulfur in the early lithiation process which leads to the effect of capacity attenuation.[25] Some active material cannot contribute to successive electrochemical reactions lead to the formation of Li_2S and Li_2S_2.[37] The insulating Li_2S and Li_2S_2 cause the loss of active material and degradation in the capacity of the composite cathode. The discharge capacities and capacity fading rate of the SMC1 composite electrode decrease with increasing cycle number. In addition, the coulombic efficiency of the composite electrodes gradually decreases in the initial 10 cycles and then remains at approximately 93%.[38]

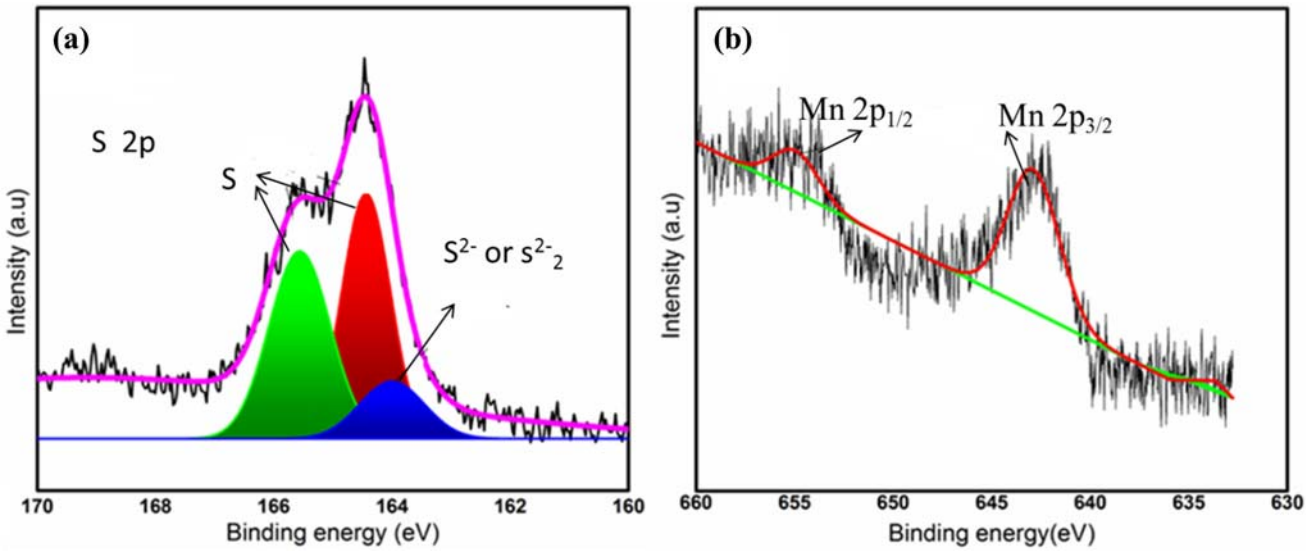

Figure 4. (a) XPS spectra for (a) S 2p and (b) Mn 2p.

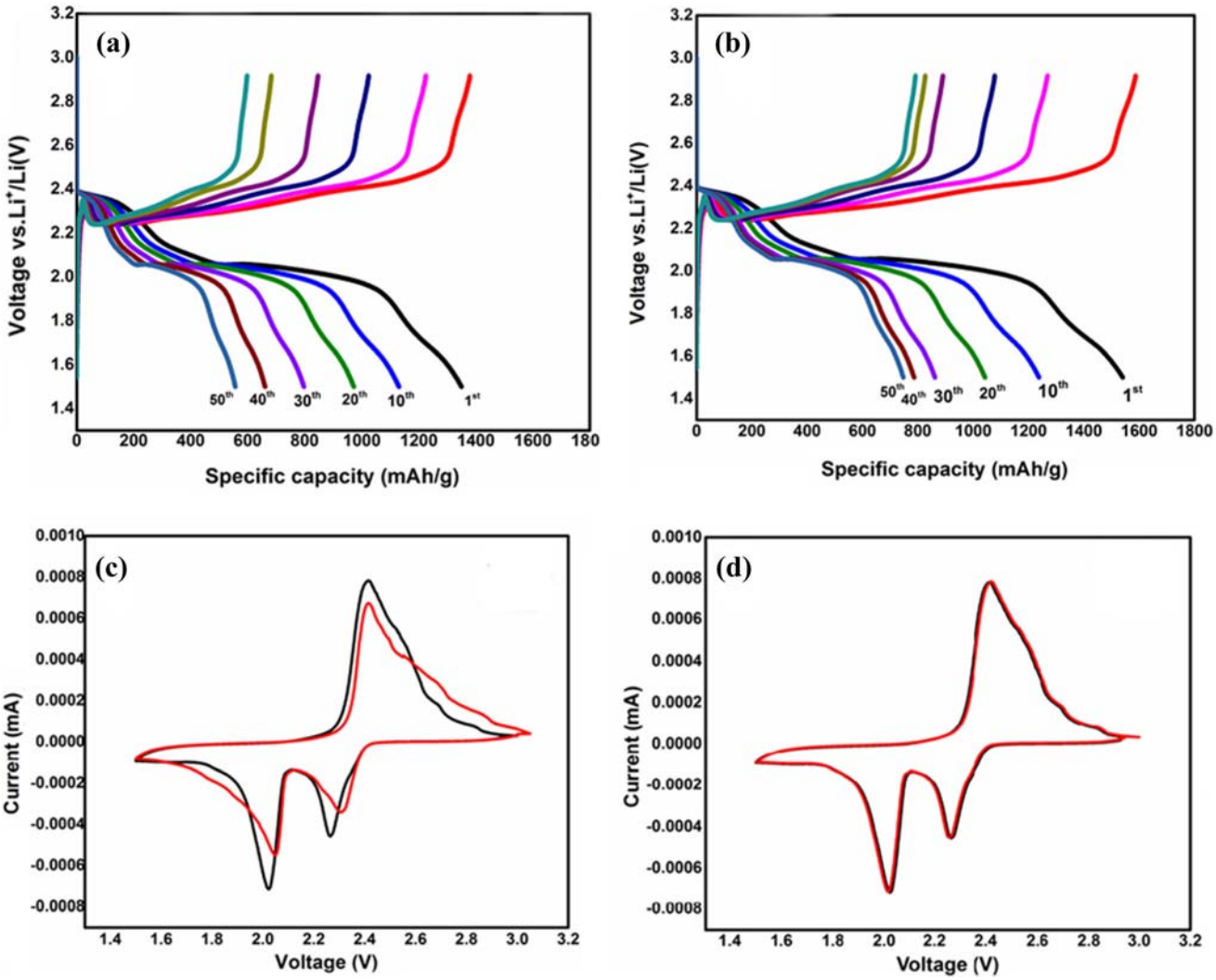

Figure 5. Galvanostatic charge–discharge curves (a) SMC1 and (b) SMC2 composite at a scan rate of 0.1C, Cyclic Voltammogram of initial and 5th cycle of (c) SMC1 and (d) SMC2 composite at a scan rate of 0.1 C.

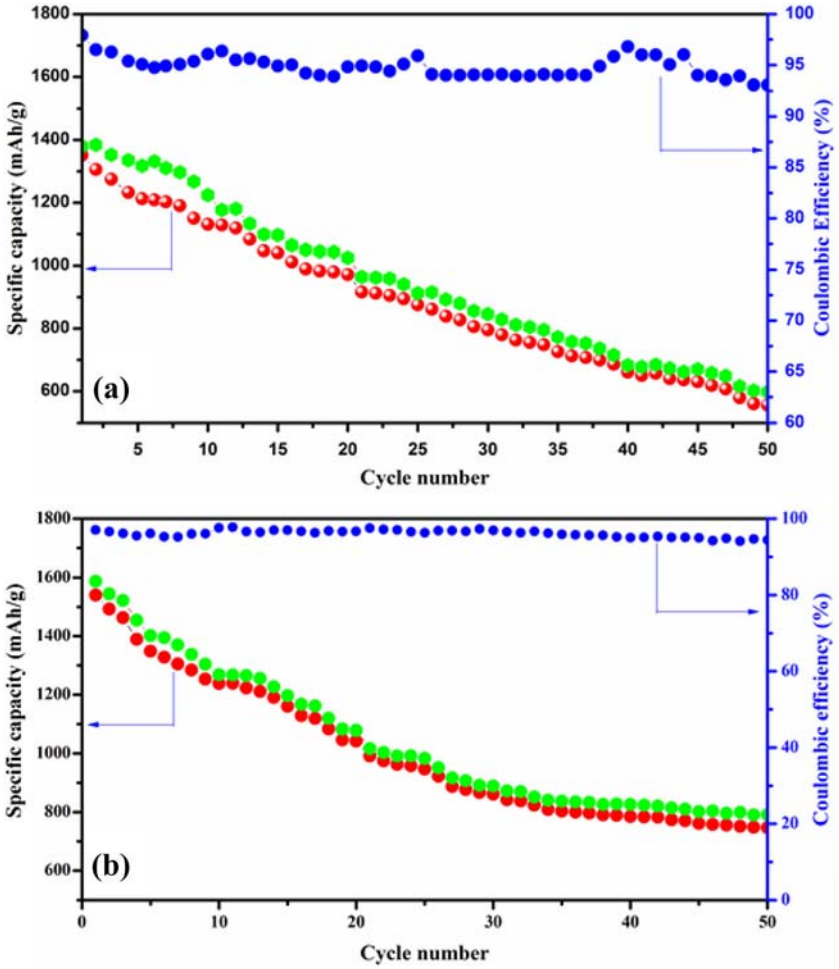

Figure 6. Coulombic efficiency of (a) SMC1 and (b) SMC2 composite.

Figure 5(b) shows that the charge capacity and discharge capacities of the SMC2 composite for an initial cycle, 10th, 20th, 30th, 40th and 50th cycles, respectively. The charge capacity is greater than the discharge capacity, which is attributed to the reactions between the dissolved lithium polysulfide intermediates and the lithium electrode.[39] The specific capacity of the composite decreases from 1540 mAh g^{-1} in the initial cycle to 1492 mAh g^{-1} in the second cycle due to irrevocable capacity loss. After the second cycle, the average fading rate was reduced and the capacity was sustained to constant at 649 mAh g^{-1} after the 50th cycle. This is concomitant with that the carbon eases the formation of small sulfur molecules in its micropores while mesoporous MnO_2 act as a shield layer to avert the outflow of sulfur during cycling gives rise to excellent cyclic stability.

Figure 5(c) illustrates the cyclic voltammogram performance of the SMC1 and SMC2 composites cathode at its initial cycle and 5th cycle. The peaks observed at higher reduction potentials attributes to the conversion of elemental sulfur (S8) to higher-order lithium polysulfides (Li_2S_x, $4 \leq x \leq 8$), while the peak at low reduction potential associated to the reduction of higher-order polysulfides to insoluble lithium polysulfides, such as Li_2S_2 and Li_2S.[19,41] The peak in the anodic scan, attributed to the oxidation of insoluble polysulfides (Li_2S and Li_2S_2) to higher-order lithium polysulfides and elemental sulfur (S_8).[27,28,40] In the 5th cycle of the SMC1 composite, reduction peaks are shifted to the high potential region; it indicates relocation of the emigrating active material to electrochemically favorable positions.[41] From Figure 5(d) SMC2 composite electrode exhibits two potential plateaus in the range of 2.25 and 2.0 V is observed in an initial cycle and its 5th cycle at 0.1 C. The internment of sulfur in the pores of MnO_2 minimizes the loss of lithium polysulfides to the electrolyte and prohibits shuttling. The partially graphitic character of the carbon is affirmed to provide the mechanical stability to the electrode and support good transport of electrons.[42,44]

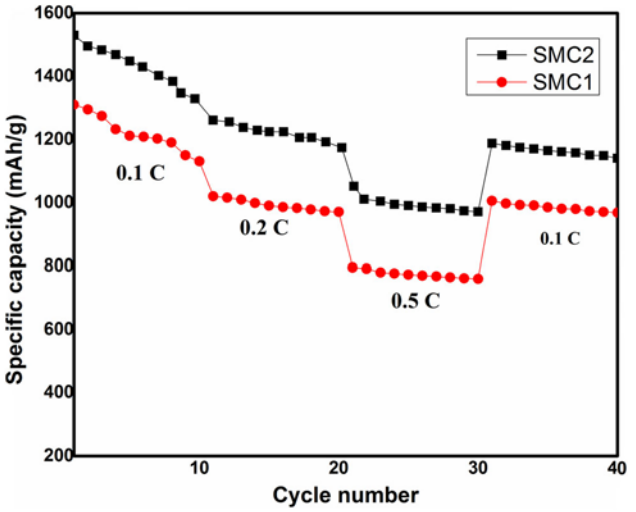

Figure 7. Rate performance SMC1 and SMC2 composite.

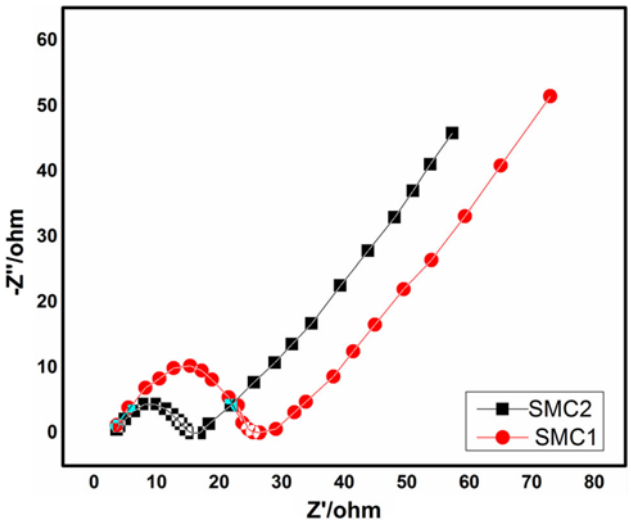

Figure 8. Nquist plots of SMC1 and SMC2 composite.

From Figure 6(a), the coulombic efficiency of SMC1 composite for the first 10 cycles of the composite is very low which can be due to the intensified impact of shuttling polysulfides resulting from the direct diffusion of some active sulfur on the surface of the composite into the electrolyte. From Figure 6(b), the coulombic efficiency of SMC2 cathode in the 50th cycle is computed to be 95%. It is clear that the composite is favorable for repeated cycling and can efficiently detain polysulfide anion diffusion in the electrolyte.[32] The superior performance of SMC2 composite is ascribed to the channel for rapid electron and ion transportation, but also restrain soluble polysulfides and suppress the "shuttle effect".[43]

However, SMC2 composite material displays the maximum initial discharge and reversible capacity owed to the existence of (i) strong sulfur/carbon interaction, (ii) strong adsorption of mesoporous MnO_2, results in a sulfur utilization and low polysulfide dissolution. The high reversible capacity is achieved not only the presence of carbon but also the strong adsorbent behavior of MnO_2 which prevents the dissolution of sulfur into the electrolyte.[26]

Rate performance of the SMC1 and SMC2 composites is also measured at different rates from 0.1 to 0.5 C and recovering at 0.1 C, as shown in Figure 7. The capacity of 1540 mAh g^{-1}, 1261 mAh g^{-1}, 1051 mAh g^{-1} and 970 mAh g^{-1} was measured at 0.1 C, 0.2 C and 0.5 C, respectively. The current density suddenly changed back to 0.1 C, the capacity of 1187 mAh g^{-1} was renewed, indicating the excellent reliability and stability of the SMC2 electrode. It is quite obvious that SMC2 electrode revealed much higher specific capacities for all applied current densities as compared to SMC1 electrode with the capacity of 1310 mAh g^{-1}, 1020 mAh g^{-1}, 970 mAh g^{-1} and 796 mAh g^{-1} at 0.1 C, 0.2 C and 0.5 C, respectively.[45]

Electrochemical impedance spectroscopy (EIS) measurements of the SMC1 and SMC2 composites were carried out and shown in Figure 8. The semicircle in the high-frequency region is attributed to the charge-transfer process occurring at the electrolyte–electrode interface and the straight line (Warburg impedance) in the low-frequency region is related to semi-infinite diffusion. Noticeably, the charge transfer resistance (Rct) of the SMC2 composites are much lower than SMC1 composite. Therefore, SMC2 composite can significantly enhance the electrical conductivity of the electrode and accelerate electron transfer during the lithiation process.[46]

4. Conclusions

In summary, the SMC1 and SMC2 composite cathode materials were successfully prepared by a simple heat treatment method. The SMC2 composite showed an initial discharge capacity of 1540 mAh g^{-1} at a scan rate of 0.1 C. Moreover, the composite material revealed that the MnO_2 has been promoted on the shallow of the composite to trap the dissolved polysulfides effectively and improve the stability of the electrode, which leads to enhanced performance for the lithium−sulfur battery. The MnO_2 and AB retain the pathways for electrolyte/Li^+ insertion in the pores of cathode material and adsorb the polysulfides and suppress the diffusion of polysulfides into the electrolyte which makes a highly promising cathode material for lithium−sulfur batteries.

Supplementary Information (SI)

Figure S1–S3 are available at www.ias.ac.in/chemsci.

Acknowledgements

All the authors from Alagappa University acknowledge the financial support by DST-SERB, New Delhi under the Physical sciences, grant sanctioned *vide* EMR/2016/006302. Also, all the authors gratefully acknowledge for extending the analytical facilities in the Department of Physics, Alagappa University under the PURSE and FIST programme, sponsored by Department of Science and Technology (DST) New Delhi, Govt. of India and Ministry of Human Resource Development RUSA- Phase 2.0 grant sanctioned vide Lt.No. F-24-51/2014 U Policy (TNMulti Gen), Dept. of Education, Govt. of India.

References

1. Pang H D, Yang Z X, Lv J, Yan W H and Guo T L 2014 Novel MnOx@Carbon hybrid nanowires with core/shell architecture as highly reversible anode materials for lithium ion batteries *Energy* **69** 392
2. Yang Z, Meng Q, Guo Z, Yu X, Guo T and Zeng R 2013 Highly reversible lithium storage in uniform $Li_4Ti_5O_{12}$/carbon hybrid nanowebs as anode material for lithium-ion batteries *Energy* **55** 925
3. Bruce P G, Freunberger S A, Hardwick L J and Tarascon J M 2012 Li–O_2 and Li–S batteries with high energy storage *Nat. Mater.* **11** 19
4. Zhang X, Kong X, Li G and Li J 2014 Thermodynamic assessment of active cooling/heating methods for lithium–ion batteries of electric vehicles in extreme conditions *Energy* **64** 1092
5. Song M K, Zhang Y and Cairns E J 2013 A long-life, high-rate lithium/sulfur cell: a multifaceted approach to enhancing cell performance *Nano Lett.* **13** 5891
6. Han D, Zhang B, Xiao M, Shen P, Wang S, Chen G and Meng Y 2014 Polysulfide rubber-based sulfur-rich composites as cathode material for high energy lithium/sulfur batteries *Int. J. Hydrog. Energy* **39** 16067
7. Wang L, Han Y Z, Feng X, Zhou J W, Qi P F and Wang B 2016 Metal–organic frameworks for energy storage: Batteries and supercapacitors *Coord. Chem. Rev.* **307** 361
8. Bai L, Chao D, Xing P, Tou L J, Chen Z, Jana A, Shen Z X and Zhao Y 2016 Refined sulfur nanoparticles immobilized in metal–organic polyhedron as stable cathodes for Li–S battery *ACS Appl. Mater. Interfaces* **8** 14328
9. Yang X, Qian X, Jin L, Zhao D, Wang S, Rao D, Yao S, Shen X, Zhou Y and Xi X 2016 Mesoporous TiO_2 nanosheet with a large amount of exposed {001} facets as sulfur host for high-performance lithium–sulfur batteries *J. Solid State Electrochem.* **20** 2161
10. Peng H J, Zhang G, Chen X, Zhang Z W, Xu W T, Huang J Q and Zhang Q 2016 Enhanced electrochemical kinetics on conductive polar mediators for lithium–sulfur batteries *Angew. Chem. Int. Ed.* **55** 12990
11. Wang J W, Lv C C, Zhang Y, Deng L and Peng Z 2015 Polyphenylene wrapped sulfur/multi-walled carbon nano-tubes via spontaneous grafting of diazonium salt for improved electrochemical performance of lithium–sulfur battery *Electrochim. Acta* **165** 136
12. Zhou L, Zong Y, Liu Z L and Yu A 2016 A polydopamine coating ultralight graphene matrix as a highly effective polysulfide absorbent for high-energy LiS batteries *Renew. Energy* **9** 333
13. Qu Y, Zhang Z, Zhang X, Ren G, Wang X, Lai Y, Liu Y and Li J 2014 Synthesis of hierarchical porous honeycomb carbon for lithium−sulfur battery cathode with high rate capability and long cycling stability *Electrochim. Acta* **137** 439
14. Zhang B, Qin X, Li G R and Gao X P 2010 Enhancement of long stability of sulfur cathode by encapsulating sulfur into micropores of carbon spheres *Energy Environ. Sci.* **3** 1531
15. Li W, Zhao H, Wang J, Yao C, Wang R and Wu X 2017 Disordered mesoporous polyacenes/sulfur nanocomposites: Superior cathode materials for lithium−sulfur batteries *J. Alloys Compd.* **693** 1045
16. Song L F, Zhang J, Sun L X, Xu F F L, Zhang H Z, Si X L, Zhou H Y, Sun D L, Du Y, Cao Z and Gabelica Z 2012 Mesoporous metal–organic frameworks: design and applications *Energy Environ. Sci.* **5** 7508
17. Cakan R D, Morcrette M, Nouar F, Davoisne C, Devic T, Gonbeau D, Dominko R, Serre C, Ferey G and Tarascon J M 2011 Cathode composites for Li–S batteries via the use of oxygenated porous architectures *J. Am. Chem. Soc.* **133** 16154
18. Kumar P, Pournarab A, Kim K H, Bansal V, Rapti S and Manos M J 2017 Metal-organic frameworks: challenges and opportunities for ion-exchange/sorption applications *Progr. Mater. Sci.* **86** 25
19. Yang X, Zhu W, Cao G and Zhao X 2015 Preparation of reduced carbon-wrapped carbon–sulfur composite as cathode material of lithium–sulfur batteries *RSC Adv.* **5** 93926
20. Li G C, Hu J J, Li G R, Ye S H and Gao X P 2013 Sulfur/activated-conductive carbon black composites as cathode materials for lithium/sulfur battery *J. Power Sources* **240** 598
21. Radhika G, Subadevi R, Krishnaveni K, Liu W R and Sivakumar M 2018 Synthesis and electrochemical performance of PEG-MnO_2–sulfur composites cathode materials for lithium–sulfur batteries *J. Nanosci. Nanotech.* **18** 127
22. Lee J, Hwang T, Lee Y, Lee J K and Choi W 2015 Coating of sulfur particles with manganese oxide nanowires as a cathode material in lithium–sulfur batteries *Mater. Lett.* **158** 132
23. Du P, Wei W, Dong Y, Liu D, Wang Q, Peng Y, Chen S and Liu P 2019 Sulfur impregnation in polypyrrole-modified MnO_2 nanotubes: efficient polysulfide adsorption for improved lithium–sulfur battery performance *Nanoscale* **11** 10097
24. Rehman S, Tang T Y, Ali Z S, Huang X X and Hou Y L 2017 Integrated design of MnO_2@ carbon hollow nanoboxes to synergistically encapsulate polysulfides for empowering lithium sulfur batteries *Small* **13** 1700087

25. Li Z, Zhang J and Lou X W D 2015 Hollow carbon nanofibersfilled with MnO_2 nanosheets as efficient sulfur hosts for lithium−sulfur batteries *Angew. Chem. Int. Ed.* **54** 12886
26. Zegeye T A, Kuo C J, Wotango A S, Pan C, Chen H, Haregewoin A M, Cheng J, Suc W and Hwang B 2016 Hybrid nanostructured microporous carbon−mesoporous carbon doped titanium dioxide/sulfur composite positive electrode materials for rechargeable lithium−sulfur batteries *J. Power Sources* **324** 239
27. Ding B, Shen L, Xu G, Nie P and Zhang X 2013 Encapsulating sulfur into mesoporous TiO_2 host as a high performance cathode for lithium–sulfur battery *Electrochim. Acta* **107** 78
28. Li Q, Zhang Z, Zhang K, Xu L, Fang J, Lai Y and Li J 2013 Synthesis and electrochemical performance of TiO_2–sulfur composite cathode materials for lithium–sulfur batteries *J. Solid State Electrochem.* **17** 2959
29. Zhang Y, Zhao Y, Yermukhambetova A, Bakenov Z and Chen P 2013 Ternary sulfur/polyacrylonitrile/Mg 0.6 Ni 0.4 O composite cathodes for high performance lithium/sulfur batteries *J. Mater. Chem. A* **1** 295
30. Zhao X, Kim J K, Ahn H J, Cho K K and Ahn J H 2013 A ternary sulfur/polyaniline/carbon composite as cathode material for lithium sulfur batteries *Electrochim. Acta* **109** 145
31. Li Z, Yuan L X, Yi Z Q, Liu Y, Xin Y, Zhang Z L and Huang Y H 2014 A dual coaxial nanocable sulfur composite for high-rate lithium–sulfur batteries *Nanoscale* **6** 1653
32. Zhang B, Lai C, Zhou Z and Gao X P 2009 Preparation and electrochemical properties of sulfur–acetylene black composites as cathode materials *Electrochim. Acta* **54** 3708
33. Li Z and Yin L 2015 Nitrogen-doped MOF-derived micropores carbon as immobilizer for small sulfur molecules as a cathode for lithium sulfur batteries with excellent electrochemical performance *ACS Appl. Mater. Interfaces* **7** 4029
34. Zheng S, Han P, Han Z, Zhang H, Tang Z and Yang, J 2014 High performance C/S composite cathodes with conventional carbonate-based electrolytes in Li–S battery *Sci. Rep.* **4** 4842
35. Liang X, Hart C, Pang Q, Garsuch A, Weiss T and Nazar L F 2015 A highly efficient polysulfide mediator for lithium–sulfur batteries *Nature Commun.* **6** 5682
36. Zhou H, Yang X, Lv J, Dang Q, Kang L, Lei Z, Yang Z, Hao Z and Liu Z H 2015 Graphene/MnO_2 hybrid film with high capacitive performance *Electrochim. Acta* **154** 300
37. Evers S and Nazar L F 2012 Graphene-enveloped sulfur in a one pot reaction: a cathode with good coulombic efficiency and high practical sulfur content *Chem. Commun.* **48** 1233
38. Kong L, Handa Y and Taniguchi I 2016 Synthesis and characterization of sulfur–carbon–vanadium pentoxide composites for improved electrochemical properties of lithium–sulfur batteries *Mater. Res. Bull.* **73** 164
39. Wang C, Su K, Wan W, Guo H, Zhou H, Chen J, Zhang X and Huang Y 2014 High sulfur loading composite wrapped by 3D nitrogen-doped graphene as a cathode material for lithium–sulfur batteries *J. Mater. Chem. A* **2** 5018
40. Li Z, Jiang Y, Yuan L, Yi Z, Wu C, Liu Y, Strasser P and Huang Y 2014 A highly ordered meso@ microporous carbon-supported sulfur@ smaller sulfur core–shell structured cathode for Li–S batteries *ACS Nano* **8** 9295
41. Su Y S and Manthiram A 2012 Lithium–sulphur batteries with a microporous carbon paper as a bifunctional interlayer *Nat. Commun.* **3** 1166
42. Jayaprakash N, Surya J S, Moganty S, Corona A and Archer L A 2011 Porous hollow carbon@ sulfur composites for high-power lithium–sulfur batteries *Angew. Chem. Int. Ed.* **50** 5904
43. Guo J, Zhang J, Jiang F, Zhao S, Su Q and Du G 2015 Microporous carbon nanosheets derived from corncobs for lithium–sulfur batteries *Electrochim. Acta* **176** 853
44. Wang C, Wang X, Wang Y, Chen, Zhou H and Huang Y 2015 Macroporous free-standing nano-sulfur/reduced graphene oxide paper as stable cathode for lithium−sulfur battery. *Nano Energy* **11** 678
45. Ling B, Chen A, Liu W, Liu K, Hu H and Zhang J 2018 Simply and rapidly synthesized composites of MnO_2 nanosheets anchoring on carbon nanotubes as efficient sulfur hosts for Li-S batteries *Mater. Lett.* **218** 321
46. Ni L, Zhao G, Yang G, Niu G, Chen M and Diao G 2017 Dual core–shell structured S@C@MnO_2 nanocomposite for highly stable lithium–sulfur batteries *ACS Appl. Mater. Interfaces* **9** 34793